HYPERGRAVITY DIAGNOSTICS AND MATERIAL SYNTHESIS IN NOBLE GAS GLIDING ARC PLASMA

Lucia Potočňáková, Jiří Šperka, Pavel Souček, Petr Zikán, Job Beckers, Gerrit M.W. Kroesen, Jack J.W.A. van Loon, Vít Kudrle

Abstract

The behaviour of gliding arc discharge in argon and helium has been studied under normal gravity and hypergravity conditions. The similar influence of increased gas flow and increased gravity is reported. The measured electrical quantities show the differences between glide arc in argon and helium. Material synthesis of carbon nanomaterial has been carried out in mixture of helium with methane in both normal gravity and hypergravity.

Key words: *plasma, gliding arc, argon, helium, hypergravity, plasma-chemical synthesis, carbon nanomaterials*

1 INTRODUCTION

Plasma and electrical discharges have been a point of interest for scientists all over the world ever since the first identification of plasma. One of the best known plasma sources is an electric arc, which is known, studied and industrially employed for decades [Edels 1961]. It can be easily produced by applying the voltage high enough for gas electrical breakdown between two electrodes. After a breakdown, electric current starts to flow in previously non-conductive working gas. Due to its electrical resistance, the plasma channel is intensively heated and the difference in mass density of the heated gas in the discharge column and the cold surrounding atmosphere gives a rise to buoyant force. Buoyancy lifts the arc and it assumes a typical arc-like curved shape. However, in some electrode geometries, the plasma channel will start to slide upwards along these electrodes and thus forming a gliding arc [Fridman 1998].

The typical feature of glide arc on divergent electrodes is the repetitive character of its lifecycle. The discharge starts at the shortest distance between the electrodes, then moves up and when it reaches its maximum elongation, it extinguishes. In the very next moment, a new arc is formed again at minimal electrode distance and the whole evolution is repeated.

The gliding arc is often operated in a flow regime, when working gas is blowing into the discharge volume. The flow is usually oriented in the same direction as buoyancy. In such case, the arc is not only lifted up by buoyancy, but also a gas drag contributes to its movement and the higher the gas flow, the faster the arc moves. In that aspect, a similar effect should probably be observable if the buoyant force is increased, which can be achieved by placing the discharge into a hypergravity environment. However, the effects of hypergravity on gliding arc have never been studied before, although such study would be beneficial for deeper understanding of processes involved in all arc-like discharges and their applications.

Glide arc operated at atmospheric pressure is a plasma source exploitable in many various industrial fields in applications such as wool surface treatment, decontamination of bacterial-contaminated water [Burlica 2006, Du 2012] or dry methane reforming [Bo 2008]. As we demonstrate in this work, nanomaterial synthesis can be also performed using this type of

discharge. Although these applications are typically carried out under 1*g* conditions, they can profit from the additional knowledge gained by the study of glide arc in hypergravity. Besides, a hypergravity plasma research is of direct importance to safety precautions in space flight (high *g* levels during the take off would alter the behaviour of various forms of discharges that might arise from malfunction in electric systems), ion thrusters design or understanding of plasma related processes in atmospheres of other planets, where the gravity is significantly different from than on Earth.

This paper presents the results of experimental studies of glide arc operated in argon and helium in laboratory (normal 1g gravity) conditions as well as in hypergravity conditions achieved at Large Diameter Centrifuge (LDC) [van Loon 2008] in ESA ESTEC centre (Noordwijk, The Netherlands) during the Spin-Your-Thesis! ESA programme. Besides the diagnostics of the glide arc plasma we describe the deposition of carbon nanomaterial from methane-helium gas mixture and analyses of the deposit.

2 EXPERIMENTAL

The experimental setup (see Fig.1) used in 1*g* experiments and the experiments on LDC was the same. It was designed and constructed considering the limitations and requirements arising from its use in extreme conditions of hypergravity. The whole experimental setup had to fit inside the LDC gondola and satisfy the maximum weight restriction (80 kg). Some parts of the setup had to be controlled remotely, as the apparatus could not be accessed directly during the spinning of centrifuge.

To ensure the rigidity and robustness of the setup, we decided to fix all devices that were located inside gondola to a force-bearing steel frame with dimensions 46 cm x 38 cm x 58 cm. The frame construction provided us with three levels for mounting the devices.

The power section consisted of a variable autotransformer (variac), high-voltage (HV) transformer, high voltage probe and Rogowski coil current probe. The variac was controlled remotely (the knob of the variac was mechanically turned using a remote controlled DC motor). Its input was standard AC electric power (230 V, 50 Hz) from a socket. Its output (0%-100% of input) was applied to primary winding of HV transformer. In such way we could set suitable power to discharge also during experimental runs, with maximum available voltage of 10 kV. HV probe (Rigol RP1050H) and current probe (Pearson Elec.) were both connected to a dual channel USB oscilloscope Voltcraft DSO-2090 and provided electrical diagnostics of the discharge. Also, three data-logging multimeters (UNI-TREND UT70B, 2x UNI-TREND UT70A) and powermeter (UNI TREND UT71E) were situated on the bottom of the gondola to measure the temperature of effluent gas, effective current, effective voltage and power on the primary winding of the high-voltage transformer.

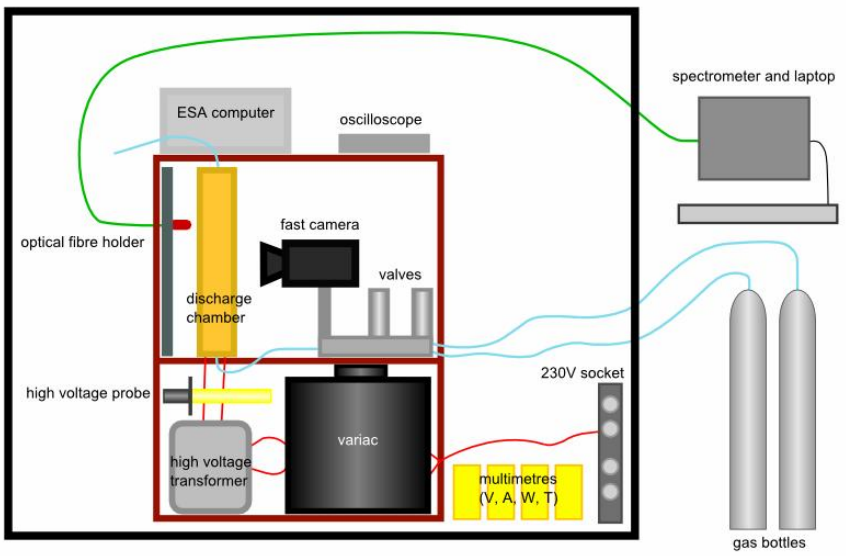

Fig. 1: *The experimental setup. Black square symbolizes the centrifuge gondola. Only the most important devices with fundamental connections (gas line, optical fibre and electrical circuit feeding the discharge) are included in the picture.*

The discharge section included the discharge chamber itself and also most of the diagnostics tools. The discharge chamber, schematically depicted in Fig. 2, had outer and inner dimensions 27x23x5 cm, 22x18x5 cm respectively. Its frame was made of spruce wood with heat resistant mica plates coating. To enable direct visual observation of the discharge, the front and back walls were made from special glass, which could resist temperatures up to 800 °C. The proper sealing protected the noble gas atmosphere inside the chamber from air impurities. The electrodes placed inside the chamber were made of copper and had a nearly quarter elliptical shape. The smallest distance between them was 4.5 mm and the initial angle was 72°.

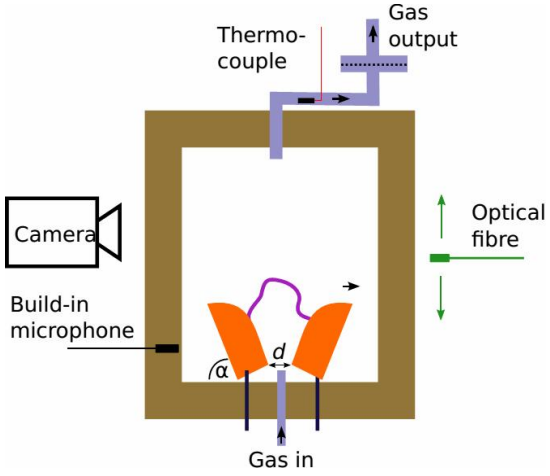

Fig. 2: *Schematic drawing of the discharge chamber with copper electrodes and diagnostic tools monitoring various properties of the discharge.*

Fast digital camera (Casio EX-ZR100) and optical fibre (connected to spectrometer Avantes Sensline AvaSpec–ULS–TEC) were located in this section for optical discharge diagnostics. Microphone for the acoustic measurements and a thermocouple (K-type) for effluent gas temperature control were integrated into discharge chamber construction.

The gas input was controlled by two calibrated needle valves, which were also included in the second section. The valves exhausted into small chamber where the mixing of gases took place in the case of two gases mixture during the material synthesis. The mixture was then fed to the discharge chamber via fused silica tube passing through wooden frame of discharge chamber. The gas exhausted through another fused silica tube, which also contained a steel mesh filter, where the nanomaterial synthesised in the discharge were collected.

The uppermost computational section included oscilloscope and hypergravity resilient industrial computer. This computer collected and saved the data from multimeters, oscilloscope, microphone and thermocouple.

Part of the experiment was located in the hub of the centrifuge – gas bottles, spectrometer and computer controlling the spectrometer. These were placed there so they are not subjected to elevated *g*-levels.

Synthesised carbon nanostructures were characterised using scanning electron microscopy (TESCAN MIRA3, 10 kV).

3 RESULTS

3.1 Visualisation of the gliding arc

The glide arc is a kind of arc discharge which is ignited between the electrodes with divergent shape. If the combination of buoyant force and gas flow drag is strong enough, such shape enables the movement of glide arc channel upwards. However, the gliding motion of the arc may appear quite different under various conditions. In following sections we will focus on describing main features of glide arc in helium and in argon.

The "gliding frequency", *i.e.* the frequency of disappearance of one arc at the highest position and consequent ignition of the new one at the shortest distance between electrodes, might be considered the main parameter of the glide arc. It contains the combined information about velocity of arc movement and the maximum height reached by the arc. However, under many conditions the gliding frequency is so high, that it limits the direct visual observation of the arc evolution. In such cases, the fast camera recordings or the photographs can be used for arc analysis.

The time resolved evolution of glide arc can be seen in Fig. 3. Argon was chosen as a working gas for this demonstration, because its gliding cycle is much more pronounced than in helium. For the discharge voltage of 4 kV, argon arc travels during its one full cycle (from ignition until quenching) the vertical distance of approximately 15 cm, while average arc in helium reaches only the height of approximately 3 cm (individual arcs may differ). It can be seen in Fig. 3, that the middle of the arc ascends faster, than the arc-electrode contact points. The middle of the arc continues to move up even after the contact points reached the top position on the electrodes (Fig. 3, approximately 500 ms after ignition).

Individual images in Fig. 3 were created by cutting the video stream into frames, so each image has 33 ms exposure time. However, thanks to the fact that the arc was AC powered, even long exposure photographs offer a possibility to visualize spatiotemporal evolution of the glide arc. With the standard AC frequency of 50 Hz (20 ms period), the arc dims (or completely disappears) and brightens each 10 ms. This effect then creates a typical striped structure, which can be seen in Fig. 4. The exposition time of the photograph in Fig. 4 is 1 s and the conditions are the same as for arc in Fig. 3. The gliding cycle in Fig. 3 took 733 ms and consistently with that, more than one full cycle is captured in Fig. 4. - the second arc overlays the first one at the bottom. This way of visualisation also reveals that in the region

between the electrodes, the arc is shaped more regularly and remains confined in one plane. After its rise above the electrodes, the arc expands also in front of and behind this plane, randomly forming the 3-dimensional structures. As gliding arc in helium never ascended above the electrodes during our experiments, it exhibited more regularity than the argon one.

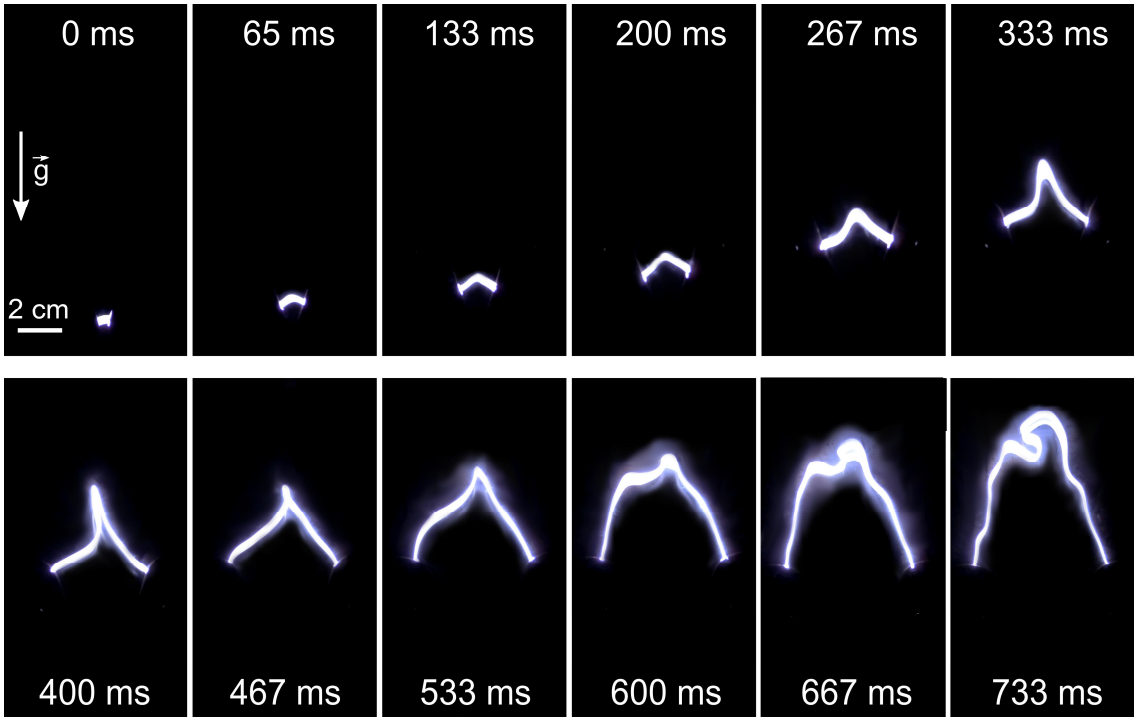

Fig. 3: *The time resolved evolution of glide arc in argon (argon gas flow 0.4 slm; discharge voltage 4kV; 1g).*

The gas flow has a huge impact on regularity of gliding arc. For low or none gas flow, the dominant force driving the gliding motion of arc is buoyancy. However, when increasing the gas flow, the drag of arc by fast moving upstream gas may outweigh the buoyancy. The drag is most intense at the bottom part, while its influence is continuously reduced at higher positions.

The sequence of three photographs demonstrating the influence of gas flow on gliding arcs can be seen in Fig. 5. The arc is maintained in argon with discharge voltage 2.8 kV (not enough for arc to expand beyond the electrode region). The exposure time of all three photographs is the same – 1/5 s, but gas flow increases significantly from left to right image. In the left image, the arcs are regularly shaped and mainly lifted up thanks to buoyancy. In the middle image, the gas flow is higher and the shape of arc is irregular and turbulent, deformed by the gas flow, which unevenly lifts it. The gas flow is even higher at right image. The frequency of appearing and quenching of individual arcs is so high here, that the shape reminds a torch and individual arcs are not even observable in this image (although they are confirmed by fast camera).

Fig.4: *Long exposure (1 s) photograph of glide arc in argon (argon gas flow 0.4 slm; discharge voltage 4 kV; 1g).*

Fig. 5: *Photographs (exposure 1/5 s) of glide arc in argon demonstrating the influence of gas flow (argon gas flow from left to right 0.4 slm, 1 slm, 2 slm; discharge voltage 2.8 kV; 1g).*

3.2 Electric properties of gliding arc in argon and helium

The computer-connected multimeters allowed us to measure and log the voltage, current and power at primary winding. The variable parameter, which was directly and continually controlled, was the primary voltage [U_p]. In following paragraphs we will discuss the trends of primary current [I_p], power [P] and power factor [cos φ] depending on primary voltage (i.e. voltage on primary winding of HV transformer) for gliding arcs in argon and in helium.

In the Fig. 6 (a) and (b), the results for gliding arcs in argon are shown. The gliding arc ascended above the electrodes for the primary voltages higher than 80 V. At this point, the sudden drop in gliding frequency occured due to nonlinearly longer distance travelled by arc. In the Fig. 6 (a), the primary current and power are plotted as functions of primary voltage. For arcs confined in the inter-electrode region, both dependencies are linear. However, after the rise of arc above electrodes at primary voltages higher than 80 V, the deflection from linearity takes place and the higher the voltage, the bigger is the deflection. The deflection is more apparent for power than for current, but the transition that the arc underwent around the primary voltage of 80 V is the most prominently displayed in Fig. 6 (b). Here, the power factor of the whole setup (i.e. not only of the plasma itself but also including both transformers) is calculated and plotted as function of primary voltage. The power factor steadily decreases for the arc in electrode region, but the trend reverses for the voltages high enough to support the arc's rising above electrodes.

The Fig. 6 (c) represents the similar situation for glide arcs burning in helium, but here the primary voltage range is significantly broader than for argon. The minimum voltage displayed in each graph in Fig. 6 corresponds to the ignition voltage in argon and helium, respectively. The ignition voltage in argon was 51 V (in terms of primary voltage; the corresponding discharge voltage was 2 kV), while arc in helium could be ignited at voltages more than twice as low (23 V primary voltage, 0.9 kV discharge voltage). The maximum voltage for an arc in argon was limited by the dimensions of the discharge chamber – the arcs at primary voltages above 110 V (at given condition) were stopped from further expansion by upper wall of the chamber. Helium, on the other hand, never extended above the electrodes and so helium gliding arcs could be operated up to primary voltage of 200 V (8 kV discharge voltage).

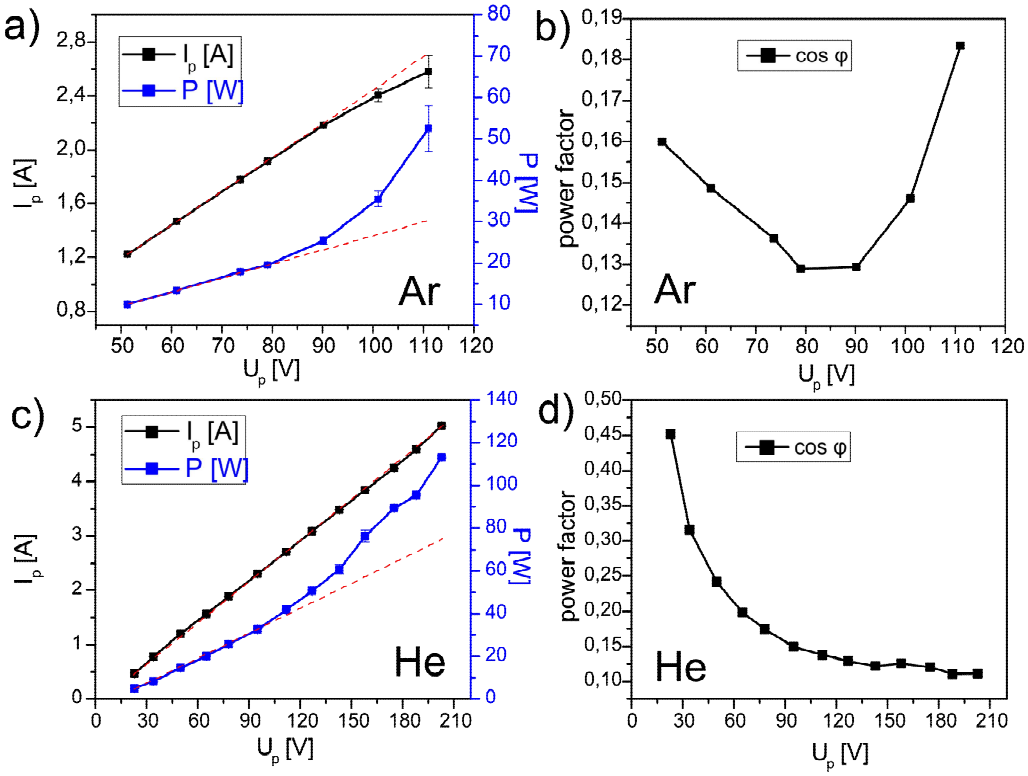

Fig. 6: *The dependency of primary current, power and power factor on primary voltage of glide arc in argon (argon gas flow 0.4 slm; 1g) and helium (helium gas flow 0.8 slm; 1g).*

Fig. 6 (d) shows corresponding power factor dependence in helium which is quite different from argon (Fig. 6 (b)). Unlike the glide arc in argon, power-factor for glide arc in helium continued to decrease during the entire range of primary voltages. The non-existence of the increasing part in the evolution of power-factor is probably related to the absence of over-electrode arc in helium.

3.3 Hypergravity diagnostics

The hypergravity experiment conducted at the Large Diameter Centrifuge in ESA ESTEC facility enabled us to achieve unique results that complement the measurements in 1*g*. The experiments focused on glide arc diagnostics as well as on material synthesis.

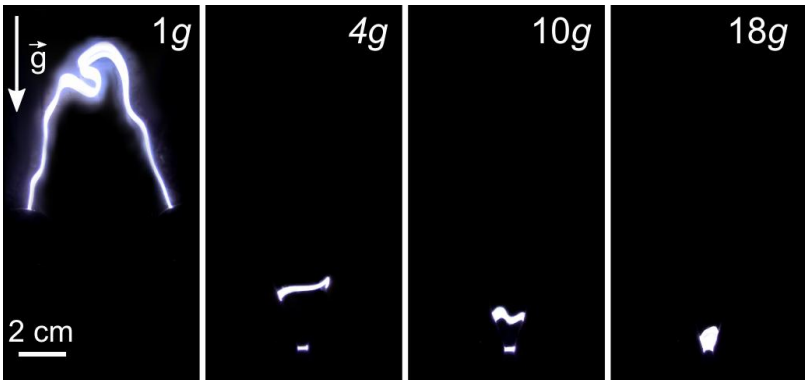

Fig. 7: *The maximum extension of a glide arc in argon before extinguishing (argon gas flow 0.4 slm; discharge voltage 4 kV; 1g, 4g, 10g, 18g).*

Fig. 7 demonstrates the influence of increased gravity on a gliding arc in argon (the situation in helium was similar, but less expressive). The individual images were obtained by the same method as in Fig. 3, but this time they do not represent the time-evolution, but a dependency of the arc's highest position (reached just before the quenching) on *g*-level. In the images of 4*g* and 10*g* a new arc forming at the bottom is already visible as well; in the image of 18*g* the whole evolution of the arc, since ignition till quenching, fitted into 33 ms time interval. The first image illustrates already known situation in 1*g*, with an arc quenching high above the electrodes. After spin-up of the centrifuge, the apparent gravitational level increased, strongly influencing the glide arc. For the gravity levels 4*g* and higher, the gliding arc was not ascending above electrodes anymore. Its length rapidly shortened, while the velocity of its movement and gliding frequency increased.

3.4 The material synthesis

The material synthesis of carbon nanomaterial has been performed from helium/methane gas mixture under both normal gravity and hypergravity conditions. The material was synthesised in the plasma and produced carbon dust particles were collected in the form of powdery material inside the discharge chamber and also on a steel mesh effluent gas filter. However, carbon deposit was also growing directly on the electrodes, forming conductive bridges between them. A typical picture of the electrodes after deposition can be found in Fig. 8 (a). Gliding arc discharge tended to transform into stable arc discharge in this case. The shortcutting of the electrodes sometimes also shortened the duration of the experiment.

In Fig. 8 (b) and (c) a typical scanning electron micrograph (SEM) of the synthesized material on the effluent gas filter can be found. Both images show the results of deposition in slightly increased gravity (2*g*). In lower magnification (Fig. 8 (b)), carbon structures with micrometer-dimension which were grown directly on the filter can be seen. The image with higher resolution (Fig. 8 (c)) shows the formation of carbon fibre.

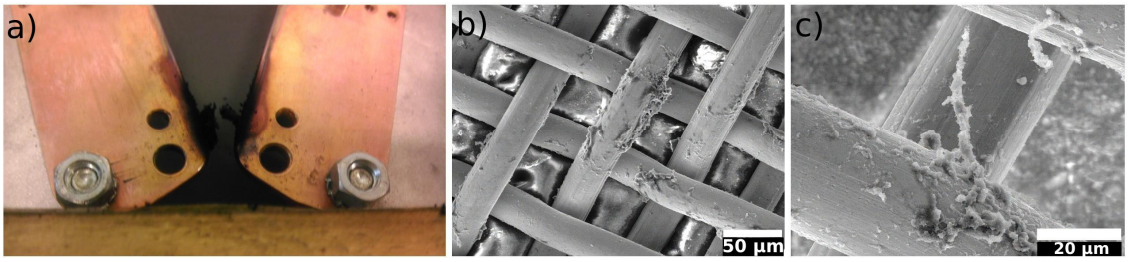

Fig. 8: *a) Typical image of copper electrodes after deposition using helium-methane mixture. b) Carbon deposit on steel mesh filter (2g), low magnification. c) Carbon deposit on steel mesh filter (2g), high magnification.*

4 CONCLUSION

In this paper, we present the experimental study of gliding arc discharge in two noble gases (argon and helium) operated under normal gravity and hypergravity conditions. The time resolved details of glide arc evolution were described based on the video stream and long exposure photograph. The increase of gas flow resulted in more turbulent and irregular shape of glide arc, higher velocity of its movement and thus also higher gliding frequency. The similar effects were observed also during increased gravity experiments. Moreover, hypergravity conditions tended to significantly shorten the maximum height reached by glide arc. While these attributes were common for glide arcs in helium and in argon, the differences between them were shown by measured electrical quantities. Additionally, material synthesis

of carbon nanomaterial has been carried out in mixture of helium with methane in both normal gravity and hypergravity, resulting in powdery material collected inside the discharge chamber and on the steel mesh effluent gas filter, which was then examined by the methods of scanning electron microscopy.

Acknowledgements

This work was supported by European Space Agency SpinYourThesis! 2012 and 2013 programmes, Masaryk University and project CZ.1.05/2.1.00/03.0086 funded by European Regional Development Fund. We would like to thank Mr. Alan Dowson from ESA-TEC-MMG for his support to these studies.

Sources

1. BO, Z., YAN, J., LI, X., CHI, Y., CEN, K. STRNAD, O., NOVÁK, L. *Plasma assisted dry methane reforming using gliding arc gas discharge: Effect of feed gases proportion.* International Journal of Hydrogen Energy 33, no. 20 (2008): 5545-5553.
2. BURLICA, R., KIRKPATRICK, M.J., LOCKE, B.R. *Formation of reactive species in gliding arc discharges with liquid water*. Journal of Electrostatics 64, no. 1 (2006): 35-43.
3. DU, Ch.M., WANG, J., ZHANG, L., LI, H.X., LIU, H., ZIONG, Y. STRNAD, O., NOVÁK, L. *The application of a non-thermal plasma generated by gas–liquid gliding arc discharge in sterilization*. New Journal of Physics 14, no. 1 (2012): 013010.
4. EDELS, H. *Properties and theory of the electric arc. A review of progress.* Proceedings of the IEEE-Part A: Power Engineering 108, no. 37 (1961): 55-69.
5. FRIDMAN, A., NESTER S., KENNEDY, L.A., SAVELIEV, A., MUTAF-YARDIMCI, O. *Gliding arc gas discharge.* Progress in Energy and Combustion Science 25, no. 2 (1998): 211-231.
6. VAN LOON, J.J.W.A., KRAUSE, J., CUNHA, H., GONCALVES, J., ALMEIDA, H., SCHILLER, P. *The large diameter centrifuge, LDC, for life and physical sciences and technology.* In Proc of the 'Life in Space for Life on Earth Symposium', Angers, France, vol. 2008. 2008.

Contact

Mgr. Lucia Potočňáková
Masaryk University, Dept. of Physical Electronics
Kotlářská 2, 611 37 Brno, Czech Republic
Tel: 549497758
email: nanai@mail.muni.cz

Mgr. Jiří Šperka, Mgr. Pavel Souček, Ph.D, Mgr. Petr Zikán, doc. Mgr. Vít Kudrle, Ph.D.
Masaryk University, Dept. of Physical Electronics
Kotlářská 2, 611 37 Brno, Czech Republic

Dr. Job Beckers, Prof. dr. ir. Gerrit M.W. Kroesen
Eindhoven University of Technology, Faculty of Applied Physics
P.O. Box 513, 5600 MB Eindhoven, The Netherlands

Dr. Ing. Jack J.W.A. van Loon
Dutch Experiment Support Center, ACTA-VU-University and University of Amsterdam
Amsterdam, The Netherlands